Available online at www.sciencedirect.com
ScienceDirect
Catalysis Today 137 (2008) 306–311
CATALYSIS TODAY
www.elsevier.com/locate/cattod

Promotion effect of Au on perovskite catalysts for the regeneration of diesel particulate filters

N. Russo, D. Fino *, G. Saracco, V. Specchia

Department of Materials Science and Chemical Engineering, Politecnico di Torino, Corso Duca degli Abruzzi 24, 10129 Torino, Italy

Available online 3 December 2007

Abstract

Four $LaBO_3$ perovskite catalysts (B = Cr, Mn, Fe and Ni), also supporting 2% by weight of gold, were prepared via the so-called *Solution Combustion Synthesis (SCS)* method, and characterized by means of XRD, BET, FESEM-EDS, TEM, O_2-TPD and CO-TPR analyses. The performance of these catalysts, in powder form, was evaluated towards the simultaneous oxidation of soot and CO. The 2 wt.% Au–$LaNiO_3$ showed the best performance with a peak carbon combustion temperature of 431 °C and a half CO conversion of 156 °C. The same nano-structured catalyst, deposited by *in situ* SCS directly over a SiC filter and tested on real diesel exhaust gases, fully confirmed the encouraging results obtained with catalyst powder.

Keywords: Diesel particulate; Perovskite catalyst; Catalytic combustion; Gold catalyst

1. Introduction

The particulates in the exhaust gases from diesel engines are a potential risk to public health. These emissions contribute to the overall suspended particulates in urban areas. However, due to their small size, they can penetrate into lungs and induce severe diseases [1]. The main targets, concerning particulate emissions control, are defined by present and future soot particulate emissions standards. Up-to-date information about these standards can be found on the web [2]. Diesel particulate filters represent the key technology to control these emissions. The filter must be regenerated periodically or continuously by burning the trapped soot in order to prevent a too high back-pressure increase [3,4]. However, the exhaust gas temperatures at the filter location often do not attain the level required for the regeneration. Therefore, auxiliary systems, such as an electrical heater or a fuel burner, must be installed to ignite trapped diesel soot. These auxiliary systems are designed to heat the exhaust gases up to the regeneration temperature (>600 °C), and consequently, this operation is exposed to a moderate risk, because of the exceptionally hot exhaust jet generated, and to some energy consumption. On the other hand, the combustion temperature of diesel particulate matter can be lowered by using a specific oxidation catalyst. The key challenge is to find a catalyst that decreases the combustion temperature of soot as much as possible so as to limit the energy requirements of periodic trap heating for regeneration purposes. Several kinds of catalysts have been tested for this purpose: perovskite type oxides [5–7], spinel type oxides [8,9], alkaline or heavy metal oxides [10–12], mixtures of halides with vanadates or molibdates [13–16] and precious metals [17]. Furthermore, during the regeneration phase of the catalytic diesel particulate filter (DPF) a high amount of carbon monoxide can be generated. Since the DPF is the last after treatment reactor in most exhaust architectures, this CO is directly emitted to the atmosphere. Hence, it should be valuable to reduce these emission by designing a multifunctional catalyst for the simultaneous abatement of soot and CO, possibly avoiding the use of Pt and Pd whose prices are both high and highly fluctuating [18]. Over the past few years supported gold catalysts gained in interest due to their surprisingly high catalytic activity towards the low-temperature CO oxidation [19–25]. The catalytic performance of gold strongly depends on the particle size, in such a way that smaller particles entail higher activities [26]. Gold-based catalysts containing nano-particles can catalyse many reactions under conditions where

* Corresponding author. Tel.: +39 011 0904710; fax: +39 011 0904699.
E-mail address: debora.fino@polito.it (D. Fino).

0920-5861/$ – see front matter © 2007 Elsevier B.V. All rights reserved.
doi:10.1016/j.cattod.2007.09.010

bulk metallic gold is inactive. Besides, it is generally known that the addition of a metal to oxides (e.g. PGMs on CeO_2 and/or La_2O_3 [27,28]) can modify the intrinsic catalytic properties of the oxides themselves, possibly increasing the activity, selectivity or stability of the obtained catalytic products. As far as the reaction mechanism is concerned, up to now it has not been well recognized if the reaction proceeds exclusively on metallic gold particles [20,29] or it might possibly occur preferentially at the edges of gold particle involving either sites on the adjacent support or on gold atoms influenced by the support [30]. Furthermore, it has been pointed out that the reaction may occur only on the support, involving adsorbed CO molecules migrated from the gold particles by spill-over and oxygen species of the support [21]. Clearly, these mechanisms could coexist. In all the cases, the interface between the gold particles and the supports plays a determinant role in the catalytic activity of the sample.

The work presented in this paper deals with the development of gold–perovskite catalysts, finally deposited on a DPF and tested on a real diesel engine, for the simultaneous abatement of soot and CO during the DPF regeneration. Beyond the catalyst itself, a key feature of this investigation lies in the innovative method used to prepare the above multifunctional catalysts (solution combustion synthesis—SCS [9]) in a single step, i.e. in a more rapid and straightforward manner than those involving a more complex *modus operandi*.

2. Experimental

2.1. Catalyst preparation and characterisation

A series of perovskite catalysts ($LaMnO_3$, $LaCrO_3$, $LaFeO_3$ and $LaNiO_3$) has been prepared according to an in-house developed method (solution combustion synthesis, SCS [9]) based on the high-exothermic and self-sustaining reactions occurring between metal nitrate precursors from an aqueous solution (acting as oxidizers) and urea (acting as a sacrificial fuel). The preparation of $LaNiO_3$ is here written as an example:

$$2La(NO_3)_3 + 2Ni(NO_3)_2 + 8CO(NH_2)_2 \rightarrow 2LaNiO_3 + 8CO_2 + 13N_2 + 16H_2O$$

The Au-based catalysts (2 wt.% Au–$LaMnO_3$, 2 wt.% Au–$LaCrO_3$, 2 wt.% Au–$LaFeO_3$ and 2 wt.% Au–$LaNiO_3$) were prepared according to the same reaction written above, by adding $HAuCl_4$ to the aqueous solutions in order to directly obtain perovskite carriers supporting 2 wt.% of gold. The catalysts were then calcined in air at 500 °C for 4 h as a common stabilisation treatment. This method, suitably adapted according to an *in situ* version, has also proved to be amenable for the deposition of mixed oxide catalysts within wall-flow diesel particulate traps based on SiC or cordierite [31].

All the catalysts were then ground in a ball mill at room temperature and characterized. X-ray diffraction (PW1710 Philips diffractometer equipped with a monochromator for the Cu Kα radiation) was used on all the fresh catalysts to examine whether the desired oxide structure was actually achieved. The specific surface area of the prepared catalyst was evaluated using a Micrometrics ASAP 2010 BET analyzer. Direct observation of the nanosized spinel crystals was performed by transmission electron microscopy (TEM-Philips CM 30 T). Conversely, a field emission scanning electron microscopy (FESEM-Leo 50/50 VP with Gemini column) and energy dispersion spectroscopy (EDS) (Hitachi, model S4700 FESEM) were used to investigate the morphology as well as the elemental composition and distribution of all the catalysts prepared.

The activity of the prepared catalyst towards soot combustion was analysed by temperature programmed combustion (TPC) carried out in a fixed bed micro-reactor, according to the standard operating procedures described in detail by Russo et al. [19]: a gas mixture (2300 ppm CO; 7 vol.% O_2; He: balance) was fed at the constant rate of 50 $Ncm^3\ min^{-1}$ to the fixed bed made of a mixture of carbon and powdered catalyst (1:9 mass basis). The analysis of the outlet gas of the reactor was performed by means of a CO_2/CO NDIR analyzer (ABB).

Finally, some oxygen temperature-programmed-desorption analyses were performed in a Thermoquest TPD/R/O 1100 analyzer, equipped with a thermal conductibility (TCD) detector. The catalysts were purged with He and then saturated with O_2 at room temperature; they were then heated up to 950 °C and the O_2 desorbed during heating was detected by the TCD detector [6]. Temperature-programmed reduction (CO-TPR) experiments were also carried out in the same apparatus. After the same oxidation pre-treatment adopted for the TPD runs, the sample was reduced with a 4.95% CO/He mixture (10 Nml/min), meanwhile heating at a 10 °C/min rate up to 950 °C. Once again, the amount of the CO converted was monitored via the TCD-MS detectors.

2.2. Catalytic trap preparation

The catalyst which showed the best performance (2 wt.% Au–$LaNiO_3$) was deposited by *in situ* SCS directly over a ceramic wall-flow filter. The filter was dipped in an aqueous solution of the catalyst precursors and then placed into an oven at 600 °C. The aqueous phase was rapidly brought to boil, the precursors mixture ignited and the synthesis reaction took place *in situ*. The support selected was a silicon carbide (SiC) filter produced by Céramiques Techniques et Industrielles (Salindres, France) (cell structure = 14/200; diameter = 58 mm; length = 150 mm; pore diameter of channel walls = 9 μm; porosity of channel walls = 40%) which was found to be chemically compatible with the catalyst. The amount of perovskites deposited was about 5 wt.%, as assessed by gravimetric analysis. The morphology of the deposited catalyst layer was analysed by FESEM observation. A foamy structure of the catalyst is indeed a pre-requisite to obtain good catalyst-to-particulate contact conditions and a rather low-pressure drop throughout the channel walls. Finally, catalyst adhesion to the monolith was assessed by a tailored ultrasonic bath test procedure [32].

2.3. Diesel engine bench tests

The developed trap was tested by means of a diesel engine bench (Kubota 1000 cc IDI engine, capable of up to 23.5 hp at 3000 rpm), where the temperature (K-type thermocouples placed at axial positions) and gas composition (Elsag-Bailey: NDIR for NO, CO, CO_2 and SO_2; FID for overall HC; paramagnetic for O_2; filtration over PALLFLEX 47 TX 40 HI 20-W filters for diesel particulate) before and after the trap can be controlled and monitored, as well as the evolution of the pressure drop (VIKA pressure transducers) through the trap, as a consequence of soot accumulation therein. A detailed description of the plant was provided by Fino et al. [32]. In line with the pending 2005 EU regulations, all the tests were carried out by using a low-sulphur diesel fuel (<50 ppmw) produced by Agip Petroli. The following standard bench test procedure was adopted: the trap was loaded by letting comparatively cold exhaust gases flow through it until a pressure drop of about 120 mbar was reached (corresponding to a soot hold-up of about 10 g l^{-1}); a "mild" regeneration [33] was then induced by post-injecting some fuel (0.08 kg/kg of exhaust gases) with a metering pump and by burning it with an oxidizing honeycomb catalyst (OXICAT by Johnson Matthey) placed just upstream the trap. The time needed for the complete trap regeneration is an index of catalyst performance as well as the completeness of soot combustion. The higher the catalyst activity the lower the required regeneration time. The progress of the regeneration process was indicated by the decrease of the trap pressure drop till a value practically equal to that measured at the beginning of the loading phase. Twin runs on virgin, non-catalytic traps were also performed for the sake of comparison.

3. Results and discussion

The XRD investigations (not shown for the sake of briefness) revealed the presence of pure and crystalline phases for all the prepared perovskites. All diffraction peaks expected according to the reference JPCDS cards ($LaNiO_3$: PDF 33-0711; $LaCrO_3$: PDF 24-1016; $LaFeO_3$: PDF 74-2203; $LaMnO_3$: PDF 89-0644) were actually observed. No secondary crystalline phases could be detected by this method, at least within the precision limits of this technique (4 wt.%). Moreover, reflections of metallic gold were always detected in the Au-based catalysts (Au: PDF 04-0784).

Figs. 1a and b show two FESEM pictures of the 2 wt.% Au–$LaNiO_3$ catalyst produced via SCS. They refer to the catalyst which showed the highest activity among those prepared, but they are quite representative of all the prepared catalysts. Most of the perovskite crystals range between 45 and 75 nm in size, which is perfectly in line with the BET specific surface areas measured and listed in Table 1 (about 20 m^2/g on average). Moreover, no indications of the possible presence of amorphous or minor crystalline phases is perceivable in Figs. 1a and b, as well as in any FESEM observations made on the prepared catalysts.

The microstructure of the catalyst crystals agglomerates looks rather spongy (Fig. 1a). This is a consequence of the sudden release of a large amount of gases during the SCS preparation, owing to the decomposition/combustion of the reacting precursors. Such a microstructure fosters the formation of highly corrugated interfaces of the catalyst powder agglomerates, which turns into an intensification of the contact between the catalyst and the soot. In the present context,

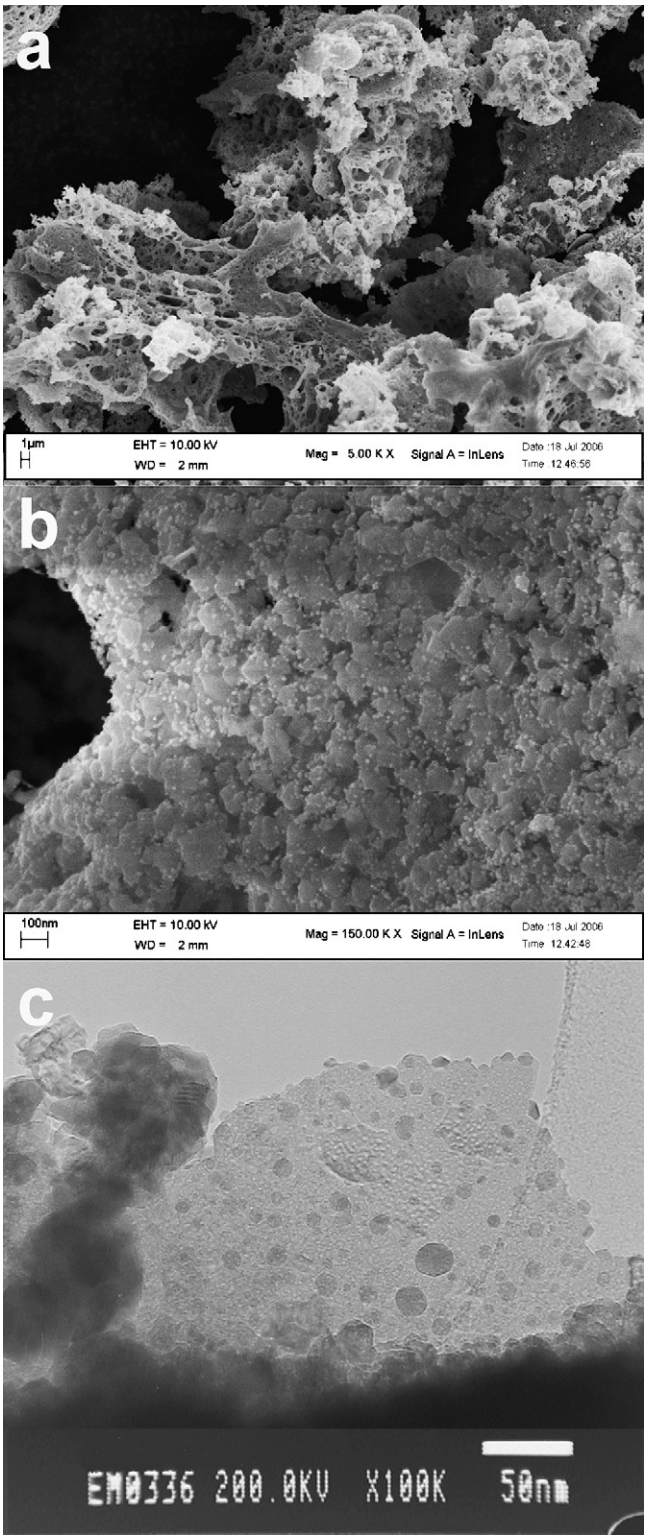

Fig. 1. FESEM views of the 2 wt.% Au–$LaNiO_3$ catalyst: (a) 5000× magnification; (b) 150,000× magnification; (c) TEM micrograph.

Table 1
Results of catalyst characterization tests: BET specific surface area and catalytic activity towards both carbon and carbon monoxide oxidation

Catalyst	BET (m^2/g)	Carbon oxidation T_p (°C)	CO oxidation	
			T_{50} (°C)	T_{100} (°C)
Non-catalytic combustion	–	650	530	>750
$LaMnO_3$	16.4	524	254	315
2 wt.% Au–$LaMnO_3$	17.7	525	234	290
$LaCrO_3$	15.8	506	450	580
2 wt.% Au–$LaCrO_3$	22.2	505	285	500
$LaFeO_3$	29.4	524	290	340
2 wt.% Au–$LaFeO_3$	18.7	525	215	240
$LaNiO_3$	14.5	430	242	280
2 wt.% Au–$LaNiO_3$	10.4	431	156	197

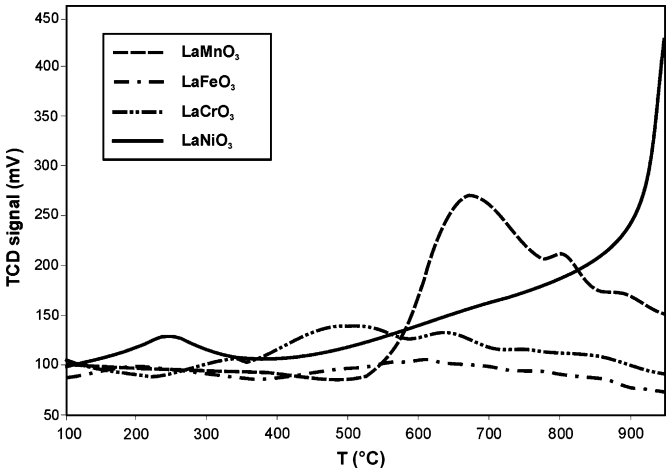

Fig. 2. Temperature-programmed oxygen desorption (TPD) plots: pure perovskite catalysts.

perovskite crystals having a size of the same order of magnitude of that of the diesel particulate aggregates (100 nm on average for the last generation of common-rail engines [34,35]) are expected to provide the highest specific number of contact points between these two counter parts. Fig. 1b shows a FESEM picture of the same catalyst but with a higher magnification in which it is possible to appreciate the good dispersion of the gold clusters deposited (the very small clearer points). Fig. 1c illustrates a TEM picture of the same 2 wt.% Au–$LaNiO_3$ catalyst. It is well representative of all the gold clusters sizes of the Au-perovskite prepared catalysts. By employing this direct observation technique values of the Au cluster size of 5–25 nm could be estimated, which are slightly larger than those obtained by more complex methods reported in literatures [36,37], which may be compensated by the fastest preparation procedure and the higher long-term stability.

Table 1 lists, beyond the BET specific surface area, the CO_2 peak temperature (T_p) in TPC experiments and both the half and total CO conversion temperature (T_{50} and T_{100}, respectively) obtained with each tested catalyst in the catalyst activity screening tests.

As expected, all the catalysts significantly lower the carbon combustion peak temperature compared with that of the non-catalytic combustion. An activity order can be outlined as follows:

- $LaNiO_3$ shows the best activity (T_p = 430 °C);
- $LaCrO_3$ is by far less active than $LaNiO_3$ (T_p = 506 °C);
- The other two-perovskite catalysts containing Mn and Fe at the B site exhibit quite similar activities (T_p = 524 °C).

This carbon combustion activity order remains substantially preserved for the perovskites containing the 2% in weight of gold. CO_2 selectivity for the catalyst-promoted combustion processes was always higher than 96%. The non-catalytic combustion of the amorphous carbon, occurring at rather high temperatures (T_p = 650 °C), was indeed found to slightly exceed 60% CO_2 selectivity.

The oxygen TPD studies were quite helpful in elucidating the catalytic activity order of the prepared catalysts. Fig. 2 shows that the $LaNiO_3$ catalyst can actually desorb the highest amount of suprafacial oxygen at rather low temperatures. This is in line with other very active perovskite catalyst whose development was dealt with in recent investigations [9], where the high catalytic activity of weakly chemisorbed oxygen species was demonstrated. Gold–perovskite catalysts provided the same oxygen desorption curves (not shown for the sake of briefness) of the corresponding pure perovskites and this behaviour is perfectly in accordance with the same catalytic performances towards carbon combustion.

Comparing the CO conversion results of the considered catalysts, in all cases the presence of gold provided a significant enhancement of the rate of carbon monoxide oxidation. The 2 wt.% Au–$LaCrO_3$ catalyst presents a higher activity than that of pure $LaCrO_3$. Considering the T_{50} values, a decrease of 165 °C (80 °C if the T_{100} is taken into account), from 450 to 285 °C, was obtained. A better performance was observed for both the $LaMnO_3$ and $LaFeO_3$ supports: the presence of gold plays once again a very positive role on the activity, as deduced from the significant reduction of the T_{50} and T_{100} values.

However, $LaNiO_3$-supporting gold showed the best performance with a T_{100} lower than 200 °C and an appreciable activity already at 100–150 °C. It is rather interesting to notice how, despite the lowest specific surface area, the $LaNiO_3$-based catalysts are delivering the best performance towards CO oxidation.

It has been reported that the nature of the support material as well as the physical state of the support can influence the catalytic activity of the resulting gold catalysts [38–40]. By comparing the results obtained with the considered catalysts (characterized by comparable Au cluster sizes) one can indeed deduce that the activity of our Au/perovskite catalysts may not result exclusively from Au, as the support itself may be involved in the reaction mechanism.

As stated earlier, some further TPR runs were performed on gold-based catalysts to possibly get further information about the nature of gold-support interaction. The results of such investigations are reported in Fig. 3. The activity order of samples is in good agreement with both the temperature at

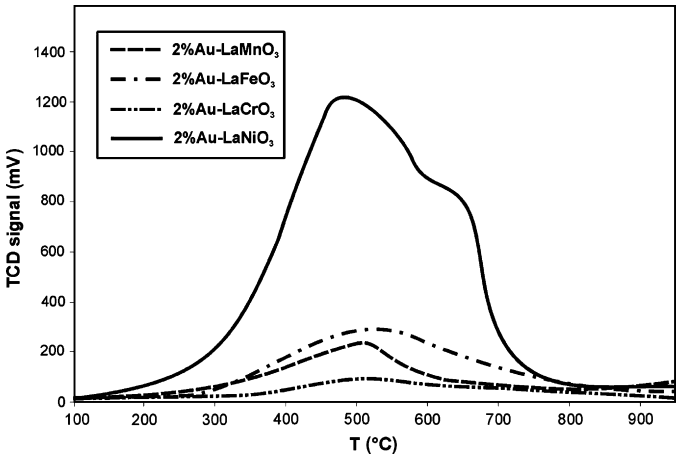

Fig. 3. CO temperature-programmed reduction (TPR) plots: Au–perovskite-type catalysts.

which CO exerts its reducing effect and, above all, the overall amount of reacted CO. The higher easiness to provide oxygen in TPR runs by gold–perovskite catalysts seems to be directly correlated with the catalytic activity. As the overall amount of oxygen reacted away in all TPR runs is different, the obtained results suggest that when the gold clusters are particularly small and with a comparable size distribution, the different catalyst surface composition can provide a different Au reacting behaviour towards CO oxidation so enlightening a different synergic effect of the perovskite supports.

Shifting to the catalytic trap topic, the most active catalyst (2 wt.% Au–$LaNiO_3$) was lined over the walls of the inlet channels of a SiC wall-flow trap so as to check the effect of its soot-CO simultaneous combustion promotion on trap regeneration under practical operating conditions. As catalyst-soot contact is expected to be a crucial issue in this context, the tailored *in situ* SCS was adopted to obtain a spongy, though well adhered, catalyst layer. Fig. 4a shows the FESEM view of the 2 wt.% Au–$LaNiO_3$ catalyst layer deposited over a SiC channel wall. As already mentioned, the microstructure is very foamy as a consequence of the sudden release of gases during the synthesis. This should potentially favour contact between the catalyst and filtered soot agglomerates thereby speeding up the combustion process during regeneration. Another positive consequence of this microstructure lies in its comparatively low-pressure drop. The thickness of the catalyst layer is in the range of 40–100 μm. Fig. 4b shows the FESEM view of the same catalytic trap but with a higher magnification. The presence of both perovskite crystals and gold clusters having the same nanostructure of the powder catalyst is a further positive results obtained by means of the *in situ* SCS. As previously underlined, catalyst crystals having a size of the same order of magnitude of that of the particulate are expected to provide the highest specific number of contact points between these two counter parts. Moreover, on the grounds of standardised vibration tests, the adhesion of the deposited catalytic layer was found to be rather good (catalyst loss lower than 0.8 wt.% after tests representative of an entire comparatively long operating lifetime of a trap [32]).

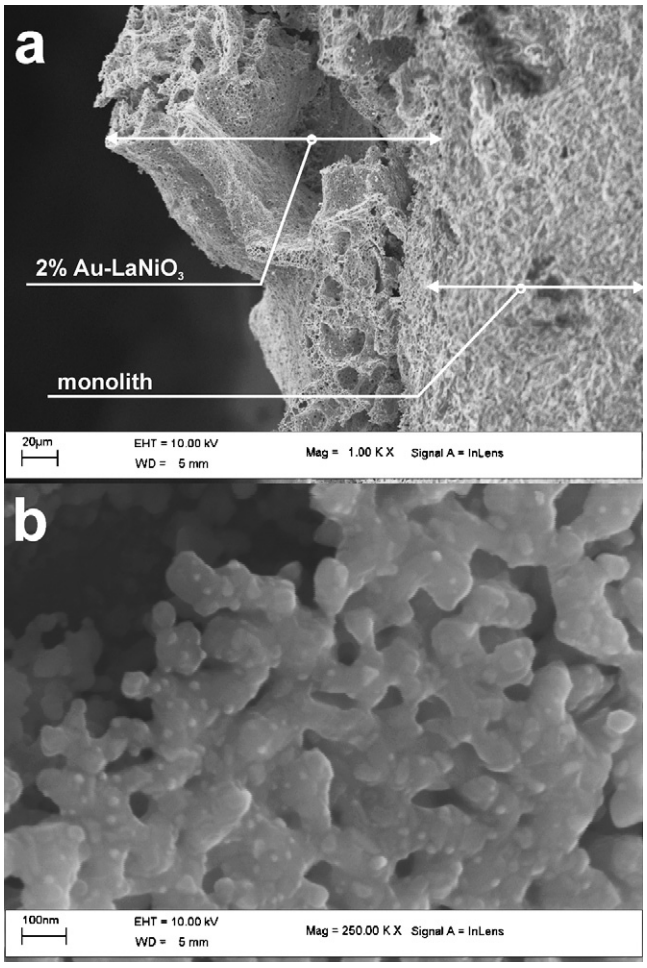

Fig. 4. FESEM view of the microstructure of a 2 wt.% Au–$LaNiO_3$ catalyst layer deposited over a SiC wall-flow trap: (a) 1000×; (b) 250,000× (the Au clusters are visible as clearer dots).

Fig. 5 compares the results of the loading and regeneration runs for the 2 wt.% Au–$LaNiO_3$-catalyzed and the non-catalyzed wall-flow traps. The results are rather encouraging. The regeneration of the catalyzed trap was much faster than that of the non-catalytic ceramic filter (threefold shorter time). Significant amount of fuel can thus be saved during filter regeneration, thereby reducing the operating costs of the soot abatement system. A Pt/Al_2O_3 commercial catalytic trap, tested under the same experimental conditions in a previous paper of ours [33], did not perform as well as the 2 wt.% Au–$LaNiO_3$-catalyzed one but still performed much better than the reference non-catalytic SiC monolith as far as the regeneration time is concerned (twofold shorter time). This statement should help the reader to contextualise the performance of the 2 wt.% Au–$LaNiO_3$-catalyzed wall-flow trap with that of a ''commercial catalyst''.

Moreover, an astonishing difference was noticed when analyzing the CO concentration during the regeneration process: the 2 wt.% Au–$LaNiO_3$ catalyst enabled a CO abatement higher than 85%, compared to the non-catalytic trap performance. This performance is also better than that of earlier tested $LaNiO_3$ traps (45% CO abatement) and of the ''commercial'' Pt/Al_2O_3 trap (70% CO abatement).

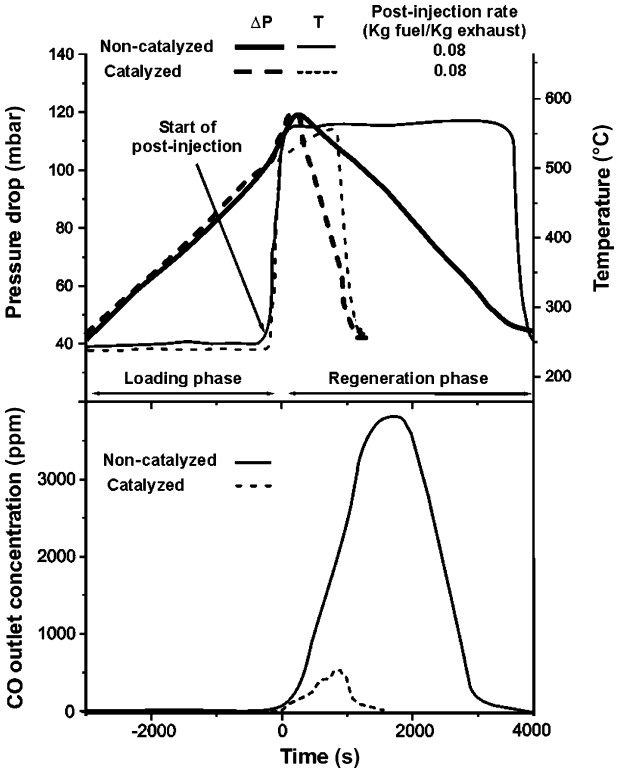

Fig. 5. Results of the loading and regeneration runs for the 2 wt.% Au–$LaNiO_3$-catalyzed and the non-catalyzed wall-flow traps.

4. Conclusions

Several perovskite catalysts ($LaMnO_3$, $LaCrO_3$, $LaFeO_3$ and $LaNiO_3$), also supporting 2% in weight of gold, were prepared by solution combustion synthesis, characterized and tested as catalysts for the simultaneous abatement of carbon and CO. The comparison of their activity with those of the corresponding pure perovskite evidenced that the presence of gold had a good synergetic effect towards CO oxidation and a negligible one towards carbon combustion. The $LaNiO_3$ perovskite exhibited the highest activity towards carbon oxidation as a consequence of its superior amount of weakly chemisorbed O^- species (α-oxygen) that were pointed out as the key players in the soot oxidation. The same catalyst supporting gold was found to be the most active towards CO oxidation because of its higher capability to provide an increased amount of oxygen to CO molecules if compared with the pure perovskite catalyst. In a subsequent effort, the best catalyst (2 wt.% Au–$LaNiO_3$) was lined over a SiC wall-flow monolith trap and tested according to a standard loading and regeneration cycle. In particular, the catalyst was found to allow a more complete regeneration compared to the non-catalytic trap in at least threefold shorter time and with a lower amount of emitted CO. An experimental test campaign is currently in progress to verify this potential under different engine operating conditions and after repeated regeneration cycles (prolonged operation).

References

[1] A. Middlebrook, J. Turner, P.A. Solomon, Atmos. Environ. 38 (2004) 5179.
[2] Summary of worldwide diesel emission standards, http://www.dieselnet.com.
[3] H. Luders, P. Stommel, R. Backes, SAE Tech. Paper no. 970470, 1997.
[4] S. Liu, A. Obuchi, J. Oi-Uchisawa, T. Nanba, S. Kushiyama, Appl. Catal. B 30 (2001) 259.
[5] Y. Teraoka, S. Kagawa, K. Nakano, W.F. Shangguan, Catal. Today 27 (1996) 107.
[6] N. Russo, D. Fino, G. Saracco, V. Specchia, J. Catal. 229 (2005) 459.
[7] D. Fino, N. Russo, E. Cauda, G. Saracco, V. Specchia, Catal. Today 114 (2006) 31.
[8] W.F. Shangguan, Y. Teraoka, S. Kagawa, Appl. Catal. B 8 (1996) 217.
[9] D. Fino, N. Russo, G. Saracco, V. Specchia, J. Catal. 242 (2006) 38.
[10] M.L. Pisarello, V. Milt, M.A. Peralta, C.A. Querini, E.E. Miro, Catal. Today 75 (2002) 465.
[11] W.F. Shangguan, Y. Teraoka, S. Kagawa, Appl. Catal. B 16 (1998) 149.
[12] A. Bueno-López, K. Krishna, M. Makkee, J.A. Moulijn, J. Catal. 230 (2005) 237.
[13] Y. Watabe, K. Yrako, T. Miyaijma, T. Yoshimoto, Y. Murakami, SAE Tech. Paper no. 830082, 1983.
[14] G. Mul, J.P.A. Neeft, F. Kapteijn, M. Makkee, J.A. Moulijn, Appl. Catal. B 6 (1995) 339.
[15] D. Fino, N. Russo, C. Badini, G. Saracco, V. Specchia, AIChE J. 49 (2003) 2173.
[16] P. Ciambelli, V. Palma, P. Russo, S. Vaccaro, J. Mol. Catal. A: Chem. 204–205 (2003) 673–681.
[17] E.S. Lox, J. Van den Tillaart, L. Leyrer, S. Eckhoff, Appl. Catal. B 10 (1996) 53.
[18] www.platinum.matthey.com/prices/index.php.
[19] N. Russo, D. Fino, G. Saracco, V. Specchia, Catal. Today 117 (2006) 214.
[20] M. Haruta, Catal. Today 36 (1997) 153.
[21] M. Haruta, S. Tsubota, T. Kobayashi, H. Kageyama, M.J. Genet, B. Delmon, J. Catal. 144 (1993) 175.
[22] J. Grunwaldt, C. Kiener, C. Wögerbauer, A. Baiker, J. Catal. 181 (1999) 223.
[23] M.A. Bollinger, N.A. Vannice, Appl. Catal. B 8 (1996) 417.
[24] M. Daté, M. Haruta, J. Catal. 201 (2001) 221.
[25] J. Grunwaldt, M. Maciejewski, O.S. Becker, P. Fabrizioli, A. Baiker, J. Catal. 186 (1999) 458.
[26] A. Wolf, F. Schüth, Appl. Catal. A 226 (2002) 1.
[27] M. Skoglundh, H. Johansson, L. Lowendahl, K. Jansson, L. Dahl, B. Hirschaauer, Appl. Catal. B 7 (1996) 299.
[28] Y.F. Yu-Yao, J.T. Kummer, J. Catal. 106 (1987) 307.
[29] F. Boccuzzi, A. Chiorino, S. Tsubota, M. Haruta, J. Phys. Chem. 100 (1996) 3625.
[30] S.D. Lin, M. Bollinger, M.A. Vannice, Catal. Lett. 17 (1993) 245.
[31] D. Fino, V. Specchia, Chem. Eng. Sci. 59 (2004) 4825.
[32] D. Fino, P. Fino, G. Saracco, V. Specchia, Chem. Eng. Sci. 58 (2003) 951.
[33] E. Cauda, S. Hernandez, D. Fino, G. Saracco, V. Specchia, Environ. Sci. Technol. 40 (2006) 5532.
[34] M. Kostoglou, P. Housiada, A.G. Konstandopoulos, Chem. Eng. Sci. 58 (2003) 3273.
[35] M. Ambrogio, G. Saracco, V. Specchia, C. van Gulijk, M. Makkee, J.A. Moulijn, Sep. Purif. Technol. 27 (2002) 195.
[36] J.R. Mellor, A.N. Palazov, B.S. Grigorova, J.F. Greyling, K. Reddy, M.P. Letsoalo, J.H. Marsh, Catal. Today 72 (2002) 145.
[37] Q. Xu, K.C.C. Kharas, A.K. Datye, Catal. Lett. 85 (2003) 229.
[38] A.I. Kozlow, A.P. Kozlova, H. Liu, Y. Iwasawa, Appl. Catal. A 182 (1999) 9.
[39] M.M. Schubert, S. Hackenberg, A.C. Van Veen, M. Muhler, V. Plzak, R.J. Behm, J. Catal. 197 (2001) 113.
[40] G.C. Bond, D.T. Thompson, Catal. Rev. Sci. Eng. 41 (1999) 319.